Int. J. Heat Mass Transfer. Vol. 17, pp. 1319-1328. Pergamon Press 1974. Printed in Great Britain

RADIATIVE HEAT TRANSFER FROM A PLASMA IN TUBE FLOW

B. D. HUNN
Department of Mechanical Engineering, Clarkson College of Technology, Potsdam, New York 13676, U.S.A.

and

R. J. MOFFAT
Department of Mechanical Engineering, Stanford University, Stanford, California 94305, U.S.A.

(*Received* 10 *September* 1973 *and in revised form* 21 *January* 1974)

Abstract—Schmidt and Leppert (1970) have reported experimental and analytical heat-transfer data for partially ionized argon flowing in a circular tube. The finite-difference model used, which was based on the then best available information, considerably underpredicted the total heat flux to the wall in the first few tube diameters.

The present study has developed a new finite-difference program, based on the Spalding–Patankar GEN program, which predicts local heat transfer for a partially ionized argon plasma flowing in a cooled, circular tube. The equilibrium radiation model incorporated in the program has been refined to include the effects of the geometry of the radiating flow field.

Experiments were conducted, using a newly developed annular radiometer, which showed the total radiation incident on the walls of the tube to be much higher than predicted. It is concluded that the discrepancy earlier reported was due to a 50 per cent underprediction of the radiative heat transfer. Non-equilibrium radiation appears to be the cause of this behavior.

NOMENCLATURE

A, area;
B, irradiation;
CRS, cylindrical receptor strip;
D, tube diameter;
f, friction factor $\tau_w/2\rho_m u_m^2$;
F, view factor;
F_{iCRSj}, view factor from emitting element to cylindrical receptor strip j;
G_∞, mass flux of main stream;
h, enthalpy referred to zero at 0°K;
j, a particular cylindrical receptor strip;
k, thermal conductivity;
$\dot{m}''$, mass flux;
Nu_x, local Nusselt number,

$$\frac{\dot{q}''D}{k(T_m - T_w)},$$

based on mixed-mean properties;
$\hat{n}$, normal vector;
$OFHC$, oxygen-free high conductivity;
P, point at center of emitting element;
P_R, volumetric radiated power;
Pr, Prandtl number;
$\dot{q}_{rad}$, radiative heat-transfer rate;
$\dot{q}''$, heat flux;
$\dot{q}''_{rad}$, radiative heat flux;
q^+, non-dimensional heat flux, $r_o\dot{q}''_w/k_oT_o$;
Re, Reynolds number;
r, radial coordinate, measured from tube centerline;
r_o, tube radius;
s, distance from emitting point to mid-plane of cylindrical receptor strip;
T, temperature;
u, velocity;
x, axial coordinate;
x^+, non-dimensional axial coordinate, $(x/r_o RePr)$;
x_o, distance from plane of emitting point to upstream edge of cylindrical receptor strip;
z, distance from emitting point to cylindrical receptor strip.

Greek symbols

β, angle in view factor geometry;
Δr, radial step width;
Δx, axial step width;
Δx_w, cylindrical receptor strip width;
θ, azimuthal coordinate;
θ_w, temperature difference $(T - T_w)$;
ω, subtended solid angle.

Subscripts

- ℄, centerline;
- e, edge;
- i, at a particular elemental fluid volume, incident;
- j, at a particular cylindrical receptor strip;
- m, mixed mean value;
- o, tube entrance;
- w, value at wall;
- x, local value.

INTRODUCTION

THE phenomenon of energy transfer from internally flowing gases at extreme temperatures is receiving increasing attention in engineering research. Specifically, the design of rocket engines, gaseous-cooled nuclear reactors, high temperature chemical processing systems, and magnetohydrodynamic power generators requires accurate knowledge of the energy transfer process between a high temperature gas and its surrounding structure. In these applications, the high energy level of the flowing gas results in extremely high temperatures, on the order of 5–10000°K. Under such extreme temperature conditions, the gas becomes ionized and often exhibits extreme property variation across short distances as well as a significant degree of thermochemical and temperature non-equilibrium. Moreover, the radiative mode of heat transfer is usually significant under these conditions.

Analytical heat-transfer results for internal flows at plasma temperatures have been presented by Incropera and Leppert [1]. Schmidt and Leppert [2] recently reported experimental heat transfer data, which included a significant radiative component, for partially ionized argon flowing in a water-cooled circular tube. They also reported predicted results for convective and total heat transfer for these same flows. However, the finite-difference scheme used considerably underpredicted the total heat transfer in the first few tube diameters.

More recent numerical studies of internal, equilibrium plasma flows, in both field and field-free regions, have been presented by Incropera *et al.* [3]. Also, Clark and Incropera [4] analytically studied the effects of non-equilibrium on both the convective and radiative heat transfer from plasmas.

None of these studies, however, includes experimental measurements of the radiative component of the total heat transfer, considered separately, although Lukens and Incropera [5] have presented radiative heat-transfer data for a plasma in the presence of an electric field, i.e. in the arc-heating region. Measurement of the radiative component of heat transfer is needed to establish the validity of the equilibrium radiation model of a field-free plasma flow. Furthermore, experimental radiation data are necessary to determine the source of the above noted discrepancy between analysis and experiment for the total heat transfer: the model of the radiation, or the model of the convection, or both.

In addition to non-equilibrium effects, inadequacies in the wall parameters used with the finite-difference procedure employed by both Incropera and Leppert and Schmidt and Leppert may be the cause of some discrepancies attributable to the convective model. Since both of these analytical procedures are based on the finite-difference scheme developed by Worsøe-Schmidt and Leppert [6], an independent approach to the finite-difference prediction method appears necessary.

In the present study the laminar flow of a plasma flowing in a cooled circular tube is solved using an adapted version of the Spalding–Patankar GEN finite-difference program [7]. The equilibrium radiation model incorporated in this program, which assumes a transparent gas and thermally black walls, has been refined to include the effects of geometry of the radiating flow field. Numerical results are presented for two of the laminar flow cases presented by Schmidt and Leppert [2]. Measurements of total thermal radiation incident on the tube walls at several axial locations are also presented. These measurements were made with an annular transpiration radiometer developed in this study.

ADAPTATION OF THE FINITE-DIFFERENCE PROGRAM

Spalding–Patankar GEN program

Spalding and Patankar [8] have developed a finite-difference program which is adaptable to laminar internal plasma flows. This program uses the von Mises transformation to introduce a non-dimensional stream function and approximates the solution with an implicit computational scheme. The original program has been modified by its authors [7] to simplify its structure and operation. The new version of the program, named GEN, incorporates a "wall function" which computes the wall parameters of shear stress and heat flux through the use of a Couette flow assumption in the wall region. This wall function was modified in the present study so as to make it compatible with application to a flowing argon plasma [9]. Adaptation of the GEN program to internal flows was also necessary.

Program qualification

To qualify the GEN program for use with laminar flow of a plasma in a tube, an extensive series of test cases was run. The reference cases were chosen from flow situations which are well established in the literature, each of which has been confirmed by experimental investigation.

Constant properties

Several cases of laminar constant property flows of air in a 1-in dia tube were run for a Reynolds number of 500. For the hydrodynamic entry length case, the predicted values of (fRe_m) agreed very closely with the analytical results of Langhaar, as reported by Kays [10].

Thermal entry length cases were run starting with a uniform temperature and a parabolic velocity profile. For the constant wall temperature case, the local Nusselt number results show agreement with analytical results presented by Kays [10], except in the early entrance region, $x^+ < 0{\cdot}01$. This discrepancy could be the result of too few terms being included in the Kays' eigenvalue solution.

For the constant heat flux case, comparison with the eigenvalue solution of Siegel *et al.* [11] was excellent (Fig. 1).

Finally, both constant heat flux and constant wall temperature results were plotted for the combined entry length problem. While the constant wall temperature results were considerably below the approximate analytical solution of Kays [10], the constant heat flux results were in close agreement with the analytical solution of Heaton *et al.* [12] (Fig. 1).

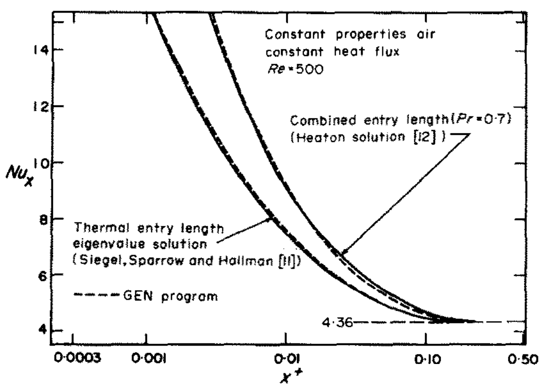

FIG. 1. Comparison of GEN program solutions with Siegel, Sparrow and Hallman and Heaton solutions for circular tube laminar entry length, constant properties air, constant wall heat flux.

Variable properties

Next, several laminar flow cases of variable properties of air for a 1-in dia tube, all for $Re = 500$, were run for both heating and cooling. Power law curve fits were used to represent the specific heat, viscosity, and thermal conductivity. Since existing experimental friction factor and heat transfer data for laminar flows with strong heating and cooling have been in agreement with the published finite-difference predictions of Worsøe-Schmidt and Leppert [6], the validity of the GEN program was tested by comparison with Worsøe-Schmidt and Leppert's results.

The first runs were for thermal entry length only, for cooling $(\theta_w = 0{\cdot}5)$ and for heating $(\theta_w = 5)$. For the cooling case, the GEN program prediction for (fRe_m) was lower by 2 per cent than that of Worsøe-Schmidt and Leppert in the $x^+ < 0{\cdot}01$ region but the two predictions coincided for $x^+ > 0{\cdot}01$. Agreement was excellent for the heat-transfer results throughout the x^+ range (Fig. 2).

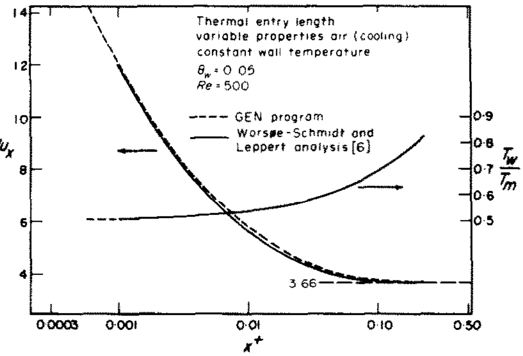

FIG. 2. Comparison of GEN program solution with Worsøe-Schmidt and Leppert numerical solution for circular tube laminar thermal entry length, variable properties air, constant wall temperature (cooling).

For the strong heating case, $\theta_w = 5$, the GEN program prediction for (fRe_m) was about 10 per cent below that of Worsøe-Schmidt and Leppert at $x^+ = 0{\cdot}001$ but was in close agreement for $x^+ \geqslant 0{\cdot}01$. Agreement for the heat-transfer results was excellent throughout the x^+ range, although the (T_w/T_m) prediction was slightly high.

Three constant heat flux cases were also run, all for heating, for non-dimensional heat fluxes q^+ of 0·5, 5 and 20. For each of these cases, agreement with the Worsøe-Schmidt and Leppert results, for both (fRe_m) and Nu_x, was excellent (Fig. 3).

Finally, a combined entry length heating case was run for constant heat flux, $q^+ = 5$. The GEN program results were compared for both (fRe_m) and Nu_x with those of Worsøe-Schmidt and Leppert and also with the numerical solution of Bankston and McEligot [13]. Agreement was very good for $x^+ \geqslant 0{\cdot}01$, but the GEN program values were slightly higher in the $x^+ < 0{\cdot}01$ region (Fig. 4).

The above quite favorable comparisons with established analyses and numerical solutions, over a wide range of heating and cooling conditions, appear to establish the validity of the GEN program model.

Plasma results based on simple radiation model

Next a series of the three cases of laminar flows of a partially ionized argon plasma presented by Schmidt and Leppert were run with the GEN program.

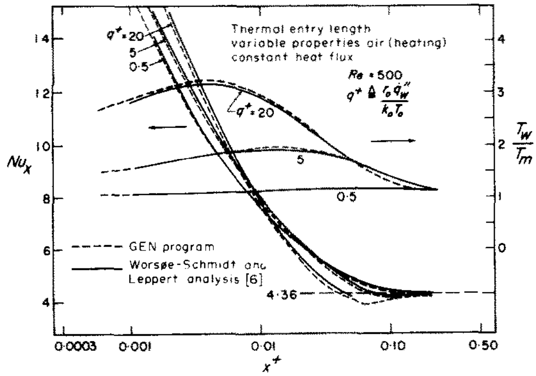

FIG. 3. Comparison of GEN program solutions with Worsøe-Schmidt and Leppert numerical solution for circular tube laminar thermal entry length, variable properties air, constant heat flux (heating).

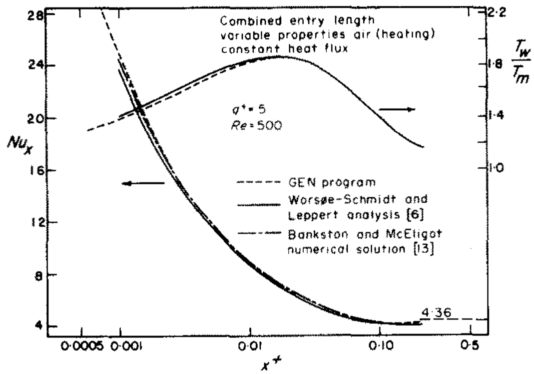

FIG. 4. Comparison of GEN program solution with Worsøe-Schmidt and Leppert numerical solution for circular tube laminar combined entry length, variable properties air, constant heat flux (heating).

These cases cover mean temperatures sufficiently high (> 11 000°K) so that in the entrance region radiation is a significant mode of heat transfer to the tube walls. In all cases, entrance velocity and temperature profiles measured by Schmidt and Leppert were used to establish starting conditions for the program. The same property values as used by Schmidt and Leppert were used: the reactive thermal conductivity of DeVoto [14] and the thermodynamic properties of Drellishak *et al.* [15] for 1 atm, equilibrium argon. The volumetric radiated power vs temperature data of Morris *et al.* of AVCO [16] for a 1 atm plasma were used as the radiation source term in the program. Typical run times were a little over 4 min on an IBM 360/67 computer.

Included in the initial computations was a radiative heat flux to the wall based on a simple model which assumes that all of the radiated energy leaves the elemental volume in the radial direction and is totally absorbed by thermally black walls. The final computations, described below, are based on a refined radiation model which takes into account the effects of the geometry of the radiating flow field.

As a check on the internal consistency of the program, a cumulative energy balance was made at each step. The final results for the three cases indicated an energy balance closure within 4·3, 2·4 and 2·5 per cent, respectively.

Figure 8 shows the results of a typical test case. It compares the wall heat flux predicted by the GEN program (convection + radiation, simple model) with the finite-difference program predictions of Schmidt and Leppert. On this same graph are the total wall heat fluxes measured by Schmidt and Leppert in a 1/2 in dia tube, for the same entrance profiles used in both finite-difference programs. As in the other two laminar test cases, the GEN program predicts the experimental data reasonably well, except in the first 3 or 4 tube diameters, where its predictions are more believable in their characteristics than are those of the Schmidt and Leppert program.

Hence, the modified GEN program is seen to operate quite well under a variety of extreme conditions. Its efficiency, reduced running time, and adaptability to turbulent flows gives it additional advantage over programs in current use.

However, although an improvement over previous techniques, the modified GEN program is not sufficient to account for the difference between analysis and experiment in the early entrance region of a confined plasma flow. Since the only major lacking of the program, besides omission of non-equilibrium effects, is that the simple radiation model does not correctly account for the direction of the emitted radiation, a refined radiation model was developed.

REFINED RADIATION MODEL

This refined model takes into account the geometry of the radiating flow field, although the constraints of a non-absorbing gas and thermally black walls are not relaxed. The program sums the contribution to the total radiative flux at the wall, at a given axial location, from all significantly radiating portions of the gas both radially and axially (both upstream and downstream). Included in the energy equation is the radiation source strength, summed over all wavelengths, at the temperature calculated by the finite-difference program for each elemental volume of gas.

Radiation is transferred from an axisymmetric finite-difference element i, in the shape of an isothermal ring of radius r_i, thickness Δr_i, and width Δx, to a small cylindrical segment of the tube wall of width Δx_w. The radiating ring is centered a distance x from the upstream edge of the cylindrical receptor strip and emits at a volumetric radiative power of P_{R_i} (W/m^3) evaluated at the element temperature T_i.

This ring is modeled as a circular line source at its center. Thus, the radiative flux incident on the receptor strip j is

$$\dot{q}''_{\mathrm{rad}_{i\to j}} = \frac{P_{R_i} r_i \Delta r_i \Delta x F_{iCRSj}}{r_o \Delta x_w} \quad (1)$$

where F_{iCRSj} is the view factor from the emitting circular line source to an arbitrary receptor strip j. The view factor geometry is illustrated in Fig. 5.

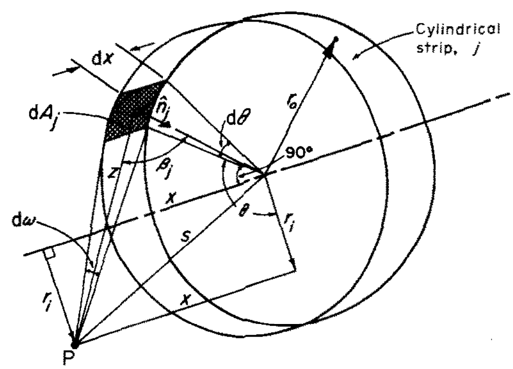

FIG. 5. View factor geometry.

The total view factor to the whole receptor strip is

$$F_{iCRSj} = F_{P\to \mathrm{d}A_j} = \int_{A_j} \frac{\cos\beta_i \,\mathrm{d}A_j}{4\pi z^2} \quad (2)$$

where $\mathrm{d}A_j = r_o \mathrm{d}\theta \mathrm{d}x$. Integrating with respect to x this becomes

$$F_{P\to A_j} = \frac{1}{2\pi}\int_{\theta=0}^{\theta=\pi}\left[\frac{\left(1-\frac{r_i}{r_o}\cos\theta\right)}{\left(1+\left(\frac{r_i}{r_o}\right)^2-2\left(\frac{r_i}{r_o}\right)\cos\theta\right)}\right.$$
$$\times\left\{\frac{\frac{x_o}{r_o}+\frac{\Delta x}{r_o}}{\sqrt{\left[\left(\frac{x_o}{r_o}+\frac{\Delta x}{r_o}\right)^2+1+\left(\frac{r_i}{r_o}\right)^2-2\left(\frac{r_i}{r_o}\right)\cos\theta\right]}}\right.$$
$$\left.\left.-\frac{\frac{x_o}{r_o}}{\sqrt{\left[\left(\frac{x_o}{r_o}\right)^2+1+\left(\frac{r_i}{r_o}\right)^2-2\left(\frac{r_i}{r_o}\right)\cos\theta\right]}}\right\}\right]\mathrm{d}\theta. \quad (3)$$

Since this expansion cannot be integrated analytically, a scheme was devised whereby $F_{P\to A_j}$ could be simply evaluated.

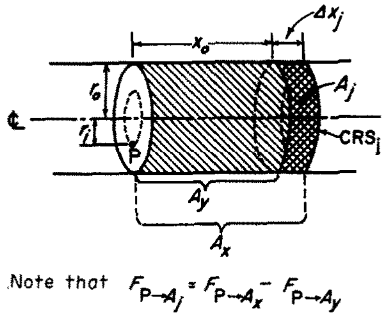

FIG. 6. View factor geometry for computation scheme.

As shown in Fig. 6, the view factor F_{iCRSj} can be computed by subtracting $F_{P\to A_y}$ from $F_{P\to A_x}$. For a given (r_i/r_o) and $(x_o/r_o = 0)$,

$$F_{P\to A_x} = F_{P\to A_j}\left(\frac{\Delta x}{r_o} = \frac{x_o+\Delta x_j}{r_o}\right)$$

and

$$F_{P\to A_y} = F_{P\to A_j}\left(\frac{\Delta x}{r_o} = \frac{x_o}{r_o}\right).$$

A plot of $F_{P\to A_j}$ vs $(\Delta x/r_o)$ for several values of (r_i/r_o) was generated, Fig. 7, numerically integrating equation (3) with $(x_o/r_o = 0)$; the plot is consulted twice, the difference yielding F_{iCRSj}.

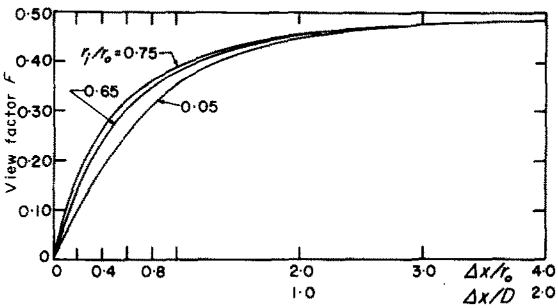

FIG. 7. Curve of view factor, F_{iCRSj}, for various r_i/r_o.

In the entrance region the tube wall is divided into receptor strips of equal width. Starting at the tube entrance the marching proceeds downstream, terminating at $(x/D = 6)$. At each axial station, the i emitting elemental rings are considered sequentially, starting at the tube centerline and proceeding toward the wall. The radiation absorbed at a given receptor strip, from an element i, is added to that contributed by all previous emitting rings. Details of the procedure are described by Hunn [17].

The general problem of calculating radiation from a confined plasma flow requires specification of an initial condition for the radiation. For tube flows this condition takes the form of a specification of the upstream radiation crossing the entrance plane. Since no measurement of this entrance plane radiation was made, it was modeled, based on measured temperature profiles at the tube entrance and assuming equilibrium in the arc-heating region. Radiation from the luminescent arc-heating core, extending 1·3 dia upstream of the entrance plane, was modeled as coming from a line source at the tube centerline. The source strength was specified as an equivalent volumetric radiative power, determined by integrating over the radiating portion of the measured entrance temperature profile, assuming this profile to be invariant with axial position in the arc-heating region. This upstream contribution was also doubled to obtain a high value for use as a sensitivity check.

Results of refined radiation model

Figure 8 shows typical refined model results for the Laminar Test Condition 4 of Schmidt and Leppert. Both nominal and high values for the radiation at the entrance plane are shown, compared with the total heat flux measured by Schmidt and Leppert. Note that even if the high entrance plane radiation estimate is more correct, its effects are confined to essentially the first two tube diameters where the total heat flux predictions are still well below the measured values. One concludes that even though the most liberal refined radiation model, assuming equilibrium both upstream and downstream of the tube entrance, predicts more realistic behavior in the first two tube diameters, the predicted total heat flux is still substantially lower than the measured values.

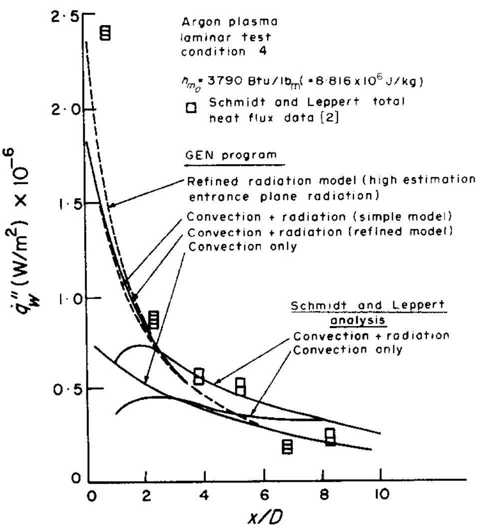

FIG. 8. Heat flux at tube wall predicted using different radiation models compared with convective heat flux and with Schmidt and Leppert analysis—plasma flow, Laminar Test Condition 4.

The question of whether the refined, equilibrium radiation model correctly predicts the radiative flux at the tube wall also remains. In order to answer this question a measurement of only the radiative component of the heat flux was made.

ARC-JET RADIATION MEASUREMENTS

Since, in a plasma, radiation reaches the wall together with mass-associated energy transfers, via convection and ambipolar diffusion, it is necessary to separate the mass-associated from the non-mass-associated energy transfers to examine the radiant portion alone. Previously available radiometer designs protect the sensor from convective effects by using windows or purged cavities but suffer the disadvantages of loss of field of view and fouling of the window. Recent research at Stanford University, however, has resulted in the successful development of a transpiration radiometer which uncouples the mass-associated energy transfer from the radiation by blowing gas through a porous sensor surface. The theory of this novel radiometer, its operating modes, and the performance of a prototype model designed for local measurements at the wall of a rectangular cross-section channel or large diameter duct is described by Moffat *et al.* [18].

In high intensity plasma applications, such as in the present study, however, the incident radiative flux level is quite high and the measurement is required at the wall of a circular tube of small diameter. In such situations an annular radiometer, operating in an "edge-cooled" mode, is better suited. The design, calibration and testing of such an annular, edge-cooled, transpiration radiometer in an argon plasma flow has been presented by Hunn and Moffat [19]. Only an outline of its operation and construction will be given here.

Annular transpiration radiometer

The annular radiometer was designed as an integral part of a segmented, water-cooled tube of 1/2 in dia and was interchangeable with any of the calorimeter segments which formed the remainder of the tube. This tube was attached directly downstream of the arc–plasma generator. Fabrication requirements dictated a minimum sensor element axial length of 1/4 in. Argon was chosen for the transpiration gas since argon is used as the plasma medium.

Figure 9 shows the features of the radiometer operation. Transpiration gas flows radially through the porous sensor disk whose edges are water cooled. This flow is adjusted to the minimum value required for the main stream boundary layer to be blown off the tube wall, insuring that only radiation reaches the sensor

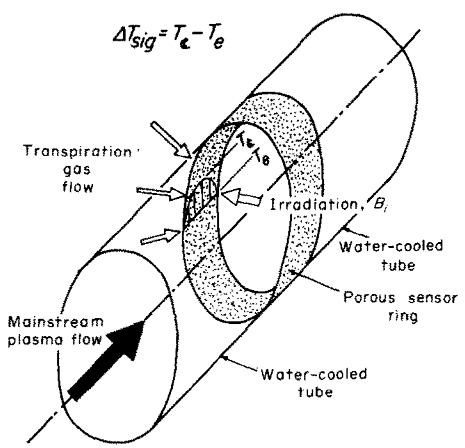

FIG. 9. Features of transpiration radiometer operation.

surface. A signal, proportional to the average radiative flux incident on the sensor, is generated between thermocouples mounted at its center and edges (in the axial direction). Through a calibration curve of ΔT_{sig} vs B_i, this signal indicates the incident radiative flux at the sensor surface and hence the tube wall.

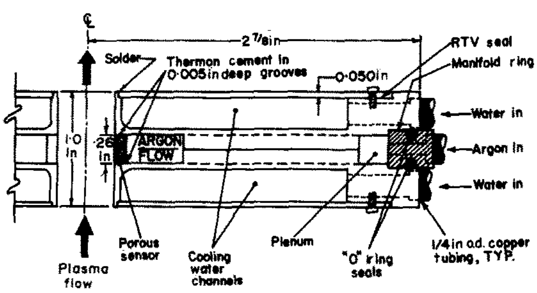

FIG. 10. Cross-section of assembled transpiration radiometer.

Figure 10 shows a cross-sectional view of the salient features of the radiometer. It is made of two 6-in dia plates machined from 1/2 in thick disks of OFHC copper. These plates are radially slotted on one side to form channels for the transpiration flow, and are milled on the other side to form cooling water channels. Each water channel is enclosed by a copper cover plate; the cooling water inlet ports are connected to the building water supply by polyflo tubing. A 1/2-in dia hole, which forms the tube through which the plasma flows, is drilled through each plate at its center and the two plates are bolted together enclosing the porous sensor ring. A manifold ring fits into a recess in both the top and bottom plates during assembly, forming a circular plenum which serves to distribute the transpiration gas circumferentially before it enters the radial slots.

The sintered bronze sensor element of 1/2 in i.d. and 0·10 in wall thickness is positioned concentrically, becoming part of the wall of the tube in which the plasma flows. Four thermocouples, for measurement of $T_{℄}$, are mounted at the inside face of the sensor ring through equally spaced holes at the midspan. At two of the midspan thermocouple positions, at both the upstream and downstream edges, are mounted thermocouples measuring T_e. The inside surface of the sensor element is sprayed with "Black Velvet" paint (Trademark, 3M Co.) of 0·95 emissivity.

Calibration was by a source "lamp" made of a spectrographic grade graphite rod, sealed in a quartz tube, and heated by a high d.c. current. A Gardon-type calorimeter, directly traceable to a National Bureau of Standards black body standard, was used as the primary calibration standard.

Preliminary testing in the arc-jet indicated the achievement of a blowoff condition at a blowing fraction $\dot{m}''/G_\infty$ of 0·07–0·09, in excellent agreement with the critical blowing fraction observed for blowoff of an isolated spot for flow in a large duct [18].

Experimental results

Final data were taken for three laminar test conditions, two of which, Laminar Test Conditions 1 and 4 [2], are presented here. The inlet centerline temperatures for these cases exceeded 12 800 and 13 300°K, respectively. Test Condition 1 is at a Reynolds number, based on entrance mixed mean temperatures, of 147 while that for Test Condition 4 is 188. Thus, both are in the laminar regime, as established by Incropera [20]. Radiative heat flux at the wall was recorded at 10, 5·5, 4 and 2·5 dia from the tube entrance, while simultaneous measurements of the total heat flux were made, using the calorimeter segments over the remainder of the tube. The results are shown in Figs. 11 and 12 where the measured radiation is indicated by the solid arrows. Also plotted are the measured total heat fluxes and those predicted by the equilibrium GEN program incorporating the refined radiation model described above.

The measured radiative flux, when added to the convective component predicted by the finite-difference program, yields the measured total heat flux, within the experimental uncertainty (±10 per cent) of the measured heat fluxes [17]. This suggests that the predicted convection is correct and that the equilibrium analytical model underpredicts, by approximately 50 per cent, the incident radiation.

The observed behavior may be partially accounted for by the fact that the calorimetric enthalpy probe temperature profile measurements at the entrance plane do not take into account non-equilibrium effects. The entrance plane temperature non-equilibrium noted in

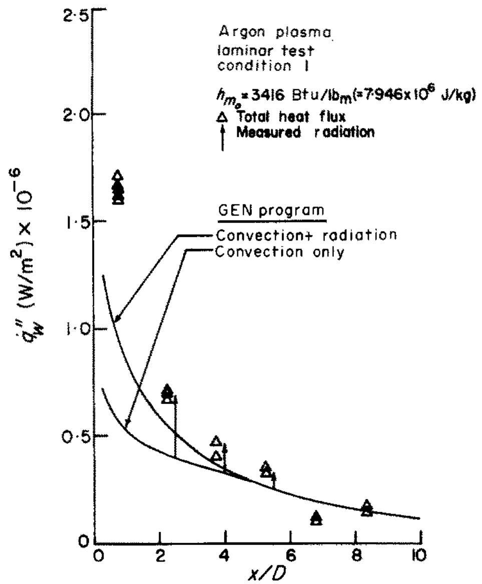

FIG. 11. Measured total radiation and measured total heat flux compared with GEN program predictions—plasma flow, Laminar Test Condition 1.

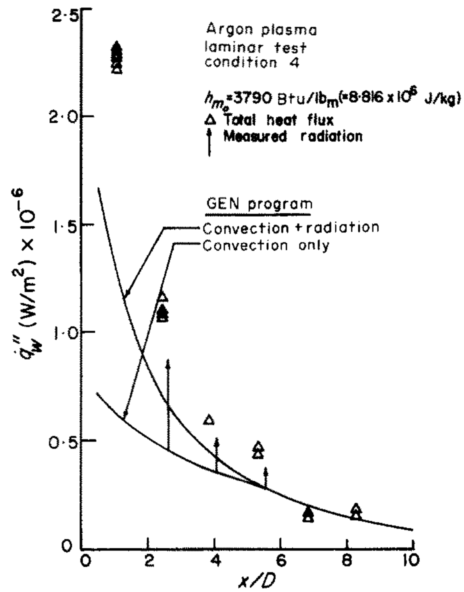

FIG. 12. Measured total radiation and measured total heat flux compared with GEN program predictions—plasma flow, Laminar Test Condition 4.

the measurements of Incropera [21] causes an underprediction of the emitted radiation, calculated to be approximately 25 per cent [17], but does not fully explain the noted behavior. The remainder of the discrepancy is evidently due to other non-equilibrium effects not accounted for in the present analytical model or in the calculation of the radiation upstream of the entrance plane.

It is possible that the equilibrium model fails to properly account for the diffusion of ionization energy through the use of a reactive thermal conductivity, as suggested by Lukens and Incropera [5]. If this is the case, a possible explanation of the results shown here, in view of the apparently correct prediction of the convection, is that the combined effects of wall-induced non-equilibrium, described by Bahadori and Soo [22], and the use of a reactive thermal conductivity, do not significantly alter the convection. However, considerable uncertainty exists concerning the effect of wall-induced non-equilibrium on convection, as is emphasized by Incropera *et al.* [3]; thus no definitive conclusion on this matter can be drawn here.

In contrast, non-equilibrium appears to strongly affect the radiation. Non-equilibrium radiation, due to temperature and thermo–chemical non-equilibrium in the arc-heating region, most likely accounts for the major portion of the high radiative heat fluxes measured.

CONCLUSIONS

The data obtained in this study show that the discrepancy between the measured and predicted total heat flux in the entrance region of a cooled tube containing a flowing plasma, which was reported by Schmidt and Leppert [2], is due to an underprediction of the total thermal radiation incident on the tube walls. Measurements of the radiation yield values nearly double the predicted values.

The refined radiation model developed here, which includes the effects of the geometry of the radiating flow field, still does not satisfactorily predict the measured radiation to the tube walls. This indicates that a significant degree of non-equilibrium exists in the upstream arc-heating region, and/or in the entrance region of plasma flows in cooled tubes, and that this non-equilibrium strongly affects the radiation emitted by the gas. A non-equilibrium model, which includes a rigorous and accurate representation of the radiation emitted from the arc-heating region, is required.

Furthermore, an accurate prediction of the convective heat-transfer behavior of partially ionized plasma flows in tubes is given by the modified Spalding–Patankar GEN program which employs a conventional finite-difference treatment of the boundary-layer equations. This program successfully treats the simultaneously developing temperature and velocity profiles and does not exhibit the anomalies occurring in the early entrance region with the modified Worsøe-Schmidt program [2].

Finally, the design of an edge-cooled transpiration radiometer has been proven feasible. This novel radiometer has been extensively qualified, calibrated, and successfully used for sustained periods in an extremely high temperature environment. It introduces a new class of instrument for radiation measurement in severe convective environments.

Acknowledgements—This paper is based on a dissertation [17] submitted to Stanford University by B. D. Hunn in partial fulfillment of the requirements for the degree of Doctor of Philosophy. The authors wish to thank Drs. W. M. Kays, C. H. Kruger and J. H. Ferziger for many useful suggestions during the course of this work. The assistance of Mr. Joseph Galate and Mr. Jay Ayers is also gratefully acknowledged. The early portions of the work were sponsored by the U.S. Atomic Energy Commission under Contract AT(04-3)-247 and the radiometer development was sponsored by the U.S. Department of the Navy under Contract N66001-70-C-0805. Funds for computer time were generously provided by the School of Engineering, Stanford University.

REFERENCES

1. F. P. Incropera and G. Leppert, Laminar flow heat transfer from an argon plasma in a circular tube, *Int. J. Heat Mass Transfer* **10**, 1861–1873 (1967).
2. P. S. Schmidt and G. Leppert, Heat transfer from plasma in tube flow, *J. Heat Transfer* **92**, 483–489 (August 1970).
3. F. P. Incropera, W. W. Bower and R. L. Kingsbury, Numerical studies of internal, equilibrium plasma flows, ASME paper 69-WA/HT-55 (1969).
4. K. J. Clark and F. P. Incropera, Thermochemical nonequilibrium in an argon constricted arc plasma, AIAA paper 71-593 (June 1971).
5. L. A. Lukens and F. P. Incropera, Electric field intensity and wall heat transfer measurements for the heating region of an atmospheric cascade arc, *Int. J. Heat Mass Transfer* **15**, 935–952 (1972).
6. P. M. Worsøe-Schmidt and G. Leppert, Heat transfer and friction for laminar flow of gas in a circular tube at high heating rate, *Int. J. Heat Mass Transfer* **8**, 1281–1301 (1965).
7. D. B. Spalding, The GEN programme for solving the equations of the two-dimensional boundary layer. Status report on 31 December, 1968, Imperial College, Mechanical Engineering Department, London, S.W.7, TR No. BL/TN/4 (December 1968).
8. S. V. Patankar and D. B. Spalding, A finite-difference procedure for solving the two-dimensional boundary layer, *Int. J. Heat Mass Transfer* **10**, 1389–1411 (1967).
9. B. D. Hunn, A finite-difference program for the prediction of argon plasma tube flows, Stanford University, Department of Mechanical Engineering, TR No. SU 247-16 (June 1971).
10. W. M. Kays, *Convective Heat and Mass Transfer*. McGraw-Hill, New York (1966).
11. R. Siegel, E. M. Sparrow and T. M. Hallman, Steady laminar heat transfer in a circular tube with prescribed wall heat flux, *Appl. Sci. Research* **A7**, 386–391 (1958).
12. H. S. Heaton, W. C. Reynolds and W. M. Kays, Heat transfer in annular passages, simultaneous development of velocity and temperature fields in laminar flow, *Int. J. Heat Mass Transfer* **7**, 763–781 (1964).
13. C. A. Bankston and D. M. McEligot, Turbulent and laminar heat transfer to gases with varying properties in the entry region of circular ducts, *Int. J. Heat Mass Transfer* **13**, 319–344 (1970).
14. R. S. DeVoto, Transport properties of partially ionized argon, *Physics Fluids* **10**, 354–364 (1967).
15. K. S. Drellishak, C. F. Knopp and A. B. Cambel, Partition functions and thermodynamic properties of argon plasma, AEDC-TR-63-146 (August 1963).
16. J. C. Morris, R. V. Krey and R. L. Garrison, Radiation studies of arc heated nitrogen, oxygen and argon plasmas, ARL 68-0103 (May 1968).
17. B. D. Hunn, Radiative heat transfer from an argon plasma in tube flow, Ph.D. Dissertation, Stanford University (May 1972).
18. R. J. Moffat, B. D. Hunn and J. F. Ayers, Development of a transpiration radiometer, Advances in Instrumentation, *Instrum. Soc. Am.* **26**, Part 2, Paper 613 (October 1971).
19. B. D. Hunn and R. J. Moffat, A transpiration radiometer for measurement of total thermal radiation from a flowing plasma, Instrumentation in the Aerospace Industry, *Instrum. Soc. Am.* **18**, 131–136 (May 1972).
20. F. P. Incropera, Flow transition phenomena in a subsonic plasma jet, Stanford University, Department of Mechanical Engineering, TR No. SU 247-9 (August 1965).
21. F. P. Incropera, Temperature measurement and internal flow heat transfer analysis for partially ionized argon, Stanford University, Department of Mechanical Engineering, TR No. SU 247-11 (August 1966).
22. M. N. Bahadori and S. L. Soo, Non-equilibrium transport phenomena of partially ionized argon, *Int. J. Heat Mass Transfer* **9**, 17–34 (1966).

RAYONNEMENT THERMIQUE D'UN PLASMA EN ECOULEMENT DANS UN TUBE

Résumé—Schmidt et Leppert (1970) ont traité expérimentalement et théoriquement du rayonnement thermique de l'argon partiellement ionisé en écoulement dans un tube. Le modèle aux différences finies, basé sur la meilleure information alors disponible, n'a pu estimer correctement le flux total thermique à la paroi, dans les premiers diamètres du tube. La présente étude développe un nouveau programme aux différences finies, basé sur le programme GEN de Spalding–Patankar, lequel calcule le transfert thermique local pour un plasma d'argon partiellement ionisé en écoulement dans un tube circulaire et refroidi. Le modèle d'équilibre du rayonnement utilisé a été amélioré pour introduire les effets de la géométrie du champ de radiation de l'écoulement.

Des expériences ont été menées à l'aide d'un nouveau radiomètre annulaire qui montre que le rayonnement total incident est, sur la paroi du tube, plus important que prévu. On conclut que le désaccord antérieur était dû à une sous-estimation du transfert thermique de l'ordre de 50 pour cent. L'absence d'équilibre du rayonnement semble en être la cause.

STRAHLUNGSWÄRMEAUSTAUSCH BEI PLASMA-ROHRSTRÖMUNGEN

Zusammenfassung—Schmidt und Leppert haben 1970 über experimentelle und analytische Wärmeübergangsdaten für in einem Kreisrohr strömendes, partiell ionisiertes Argon berichtet. Das damals auf neuesten Informationen basierende Finite-Differenzen-Modell ergab in der Anlaufstrecke erheblich zu kleine Werte für die Gesamtwärmestromdichte an die Wand.

Im Rahmen der vorliegenden Arbeit wurde ein neues Finite-Differenzen-Modell zur Ermittlung lokaler Wärmeübergangsdaten für in einem gekühlten Kreisrohr strömendes, partiell ionisiertes Argon entwickelt, das vom Spalding–Patankar-GEN-Programm ausgeht. Das dabei verwendete Gleichgewichtsstrahlungs-Modell wurde verfeinert, damit geometrische Einflüsse auf das strahlende Strömungsmodell mit berücksichtigt werden konnten. Mit einem neu entwickelten Ring-Strahlungsmeßgerät wurden Messungen durchgeführt, die bewiesen, daß die auf die Rohrwände entfallende Gesamtwärmestrahlung erheblich über den berechneten Werten liegt. Die früher beobachteten Abweichungen erklären sich durch einen in der Rechnung sich um 50% zu klein ergebenden Strahlungswärmeaustausch. Die Ursache für dieses Verhalten ist auf Nichgleichgewichtsstrahlung zurückzuführen.

ЛУЧИСТЫЙ ПЕРЕНОС ТЕПЛА ОТ ПОТОКА ПЛАЗМЫ В ТРУБЕ

Аннотация — В 1970 г. Шмидтом и Леппертом были опубликованы экспериментальные и теоретические данные по переносу тепла от частично ионизированного потока аргона в круглой трубе. Использованная при этом конечно-разностная модель, основанная на самых надежных имеющихся в то время данных, давала заниженное значение величины суммарного теплового потока на участке трубы, равном нескольким калибрам от входа.

В этой работе на основе метода Сполдинга-Патанкара разработана новая программа, использующая конечно-разностные схемы, которая позволяет рассчитывать локальный перенос тепла от потока частично ионизированной аргоновой плазмы в охлаждаемой круглой трубе. В новой программе равновесная модель излучения учитывает эффекты конфигурации потока.

Эксперименты, проводимые с использованием кольцевых радиометров новой конструкции, показали, что величина суммарного лучистого потока, падающего на стенки трубы, больше расчетного. Сделан вывод, что вышеуказанное расхождение обязано занижению лучистого переноса на 50%. Причиной этого, по-видимому, является неравновесное излучение.